Available online at www.derpharmachemica.com

ISSN 0975-413X
CODEN (USA): PCHHAX

Der Pharma Chemica, 2016, 8(8):64-72
(http://derpharmachemica.com/archive.html)

A comparative study on the structural and supercapacitive properties of TiO_2 nanotubes fabricated by potentiostatic and galvanostatic anodization

P. Shobha, D. Muthu Gnana Theresa Nathan, R. Mahesh and P. Sagayaraj*

Department of Physics, Loyola College (Autonomous), Chennai-600034, India

---

ABSTRACT

We report the fabrication of self-organized TiO_2 nanotubes employing potentiostatic and galvanostatic anodization. A comparative study is carried out to evaluate the influence of the synthetic modes on the structural and electrochemical behaviors of the samples. Structural and morphological characteristics are investigated using X-ray diffraction and field emission scanning electron microscopy. Electrochemical properties are studied by cyclic voltammetry, chronopotentiometry and electrochemical impedance spectroscopy. The sample prepared by galvanostatic approach demonstrates better capacitive performance than the sample prepared by potentiostatic mode. The enhanced electrochemical behavior is owing to tubular structure with higher accessible surface area of TiO_2 nanotubes.

Keywords: TiO_2 nanotubes, Anodization, Supercapacitor

INTRODUCTION

The ever growing energy demands motivate researchers to pursuit sustainable and renewable resources. Energy storage devices are equally significant as energy conversion systems for leveling the cyclic nature of renewable sources [1-2]. Among the energy storage devices, supercapacitors or electrochemical capacitors (ECs) have gained particular attention owing to high power density, long cycle life, and accomplish the power and energy gap between batteries and conventional electrolytic capacitors [3]. Based on the charge storage mechanism and electrode materials used, supercapacitors are categorized into two types such as electrochemical double-layer capacitors (EDLCs) and redox or pseudocapacitors [4,5]. In the case of EDLCs, carbonaceous materials are employed as electrodes whereas the pseudocapacitors employ transition metal oxides and conducting polymers. EDLCs store energy by accumulation of charges via electrostatic interaction at the electrode/electrolyte interface, while pseudocapacitors involve reversible redox reactions at the surface of electrodes [1,4-6]. Till date, hydrous RuO_2 demonstrate the best performance but its high cost limits its commercialization [7]. Therefore, the current research is redirected towards the identification of low cost electrodes based on other transition metal oxides.

Fabrication of self-organized titania nanotubes (TiO_2 NTs) on the titanium foil by electrochemical anodization has extensively been investigated. Among the other nanostructures, anodic TiO_2 NTs with unique morphology has attracted enormous interest because it can be used in functional applications such as dye-sensitized solar cells [8], gas sensors [9], lithium ion batteries [10], sodium ion batteries [11], supercapacitors [12]. Supercapacitive performance of electrode materials is mainly determined by ion diffusion kinetics, electronic conductivity and surface area [13]. Highly ordered TiO_2 NTs prepared by anodization provide improved electronic pathways and high surface area for charge storage [14]. Thus, morphology plays a crucial role in defining the performance of supercapacitor electrodes. Among the other techniques for the synthesis TiO_2 NTs, anodization method present more control in tailoring the geometry (tube diameter, tube length etc) of TiO_2 NTs [15,16]. Most of the electrochemical studies carried out on TiO_2 NTs are fabricated by potentiostatic anodization [17-18] while galvanostatic anodization is not very much investigated [19]. In the present work, self-organized TiO_2 NTs are fabricated via both

potentiostatic and galvanostatic modes. Influence of the preparative modes on the structural and electrochemical properties of TiO_2 NTs is investigated.

MATERIALS AND METHODS

2.1 Chemicals

Titanium foil (99.7%), platinum gauze, ethylene glycol, ammonium fluoride, acetone, isopropanol, ethanol and deionized (DI) water were used. All the chemicals were of high purity and no further purification was done.

2.2 Experimental methods

Titania nanotubes (TiO_2 NTs) were fabricated employing potentiostatic and galvanostatic anodization approaches. Titanium foil was utilized as working anode while platinum gauze was the counter cathode. Before anodization, the Ti foil (1.5 × 1 cm^2) was degreased by ultrasonication for 15 min with isopropyl alcohol, acetone and DI water separately and then dried in air. The back side of the Ti foil was protected by cellophane tape to prefer one sided anodization. The distance between the vertically placed electrodes was kept as 4 cm. Both the anodization processes were carried out in organic electrolytes containing ethylene glycol, ammonium fluoride (0.3 wt%) and DI water (3 vol%). During anodization process, a constant potential of 40 V (potentiostatic) and a constant current density of 2 mA/cm^2 (galvanostatic) was maintained. After 24 h of anodization, the samples were cleaned ultrasonically in ethanol to remove any surface debris. The samples were annealed at 450 ºC for 4 h. The TiO_2 NTs prepared via potentiostatic and galvanostatic modes are labeled as PT and GT, respectively.

2.3 Characterization techniques

X-ray diffractograms of the samples were recorded using a GE XRD 3003TT X-ray diffractometer with monochromatic nickel filtered CuK_α (λ = 1.5416 Å) radiation in the 2θ range of 20° to 70°. The morphology and elemental composition of the nanotubes were determined from the Carl Zeiss Supra 55 field emission scanning electron microscope (FESEM) that has the attachment of an energy dispersive X-ray analyzer (EDX). The FT-IR spectra were recorded with a Perkin Elmer Spectrum Two in the waveband of 400-4000 cm^{-1}.

2.4 Electrochemical measurements

Electrochemical performances of the samples were evaluated using Biologic VSP, France. Cyclic voltammetry (CV), chronopotentiometry (CP) and electrochemical impedance spectroscopy (EIS) measurements were carried out in a three electrode configuration, where the as-prepared TiO_2 NTs (1 cm^2), a Ag/AgCl (3 M KCl) electrode was used as reference electrode and a Pt wire as counter electrode. All the electrochemical measurements were carried out in 1 M Na_2SO_4 aqueous solution in ambient condition.

RESULTS AND DISCUSSIONS

3.1 XRD analysis

The crystallinity and phase characteristics of the samples were analyzed from powder XRD study. Fig. 1 shows the XRD patterns of TiO_2 NTs (a) PT and (b) GT. The as-anodized TiO_2 NTs were amorphous in nature. After annealing at 450 ºC, the amorphous TiO_2 NTs were transformed into anatase crystal structure which was evident from the diffraction peaks. All the reflection peaks are easily indexed to the anatase phase of TiO_2 in line with the standard JCPDS data (084-128). Absence of impurity peaks suggest that single phase TiO_2 NTs with high purity was formed. However, the peaks corresponding to Ti are also observed from the titanium substrate [20].

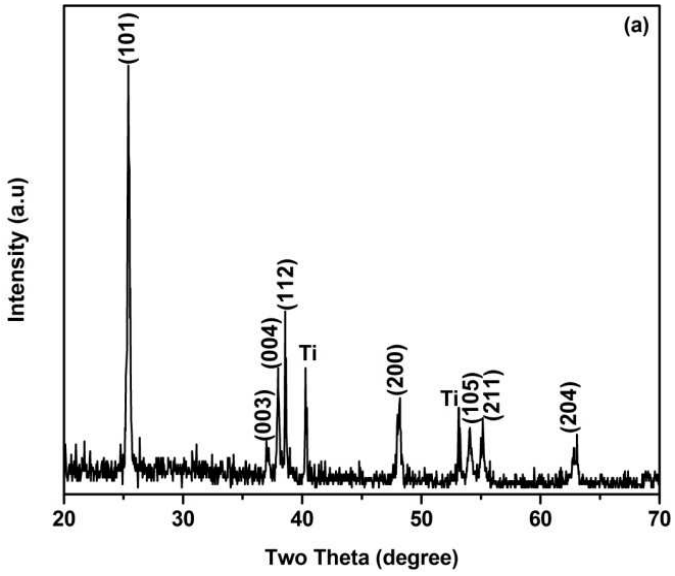

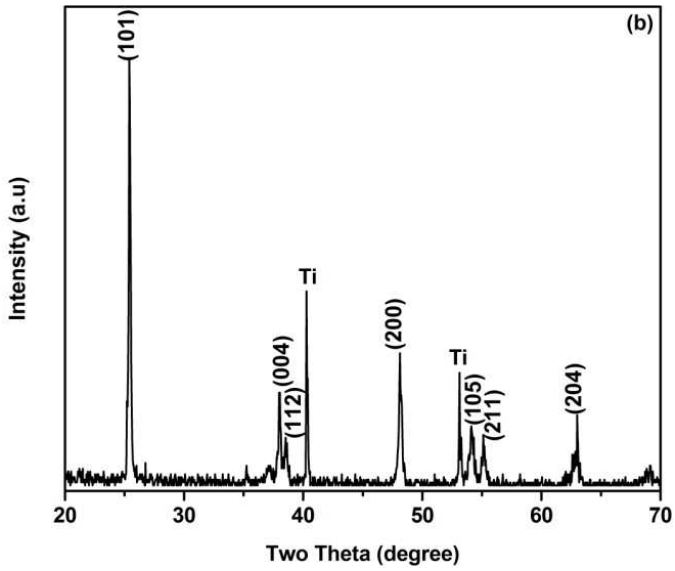

Fig. 1 XRD patterns of TiO_2 NTs (a) PT and (b) GT

3.2 FESEM analysis

The surface morphology of the as-grown TiO_2 NTs was investigated employing field emission scanning electron microscopy. FESEM micrographs of TiO_2 NTs are illustrated in Fig. 2 (PT) and Fig. 3 (GT). It is observed from the FESEM images that highly ordered TiO_2 NTs with regular porous morphology is formed. The geometrical parameters of TiO_2 NTs are presented in Table 1. In the case of potentiostatic anodization, pore diameter, wall thickness and tube length of PT are found to be 110 nm, 22 nm and 14.1 μm, respectively. Galvanostatically prepared GT showed improved geometrical parameters with pore diameter of 130 nm, wall thickness of 19 nm and tube length of 16.9 μm.

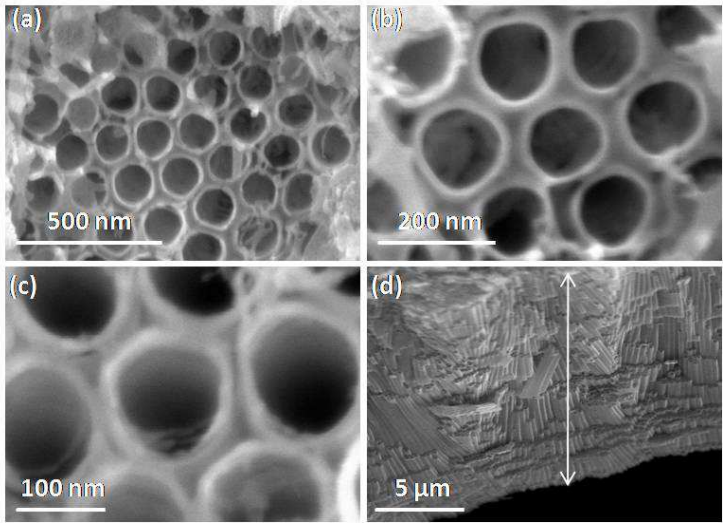

Fig. 2 FESEM images of TiO_2 NTs (a-c) top view and (d) cross-sectional view

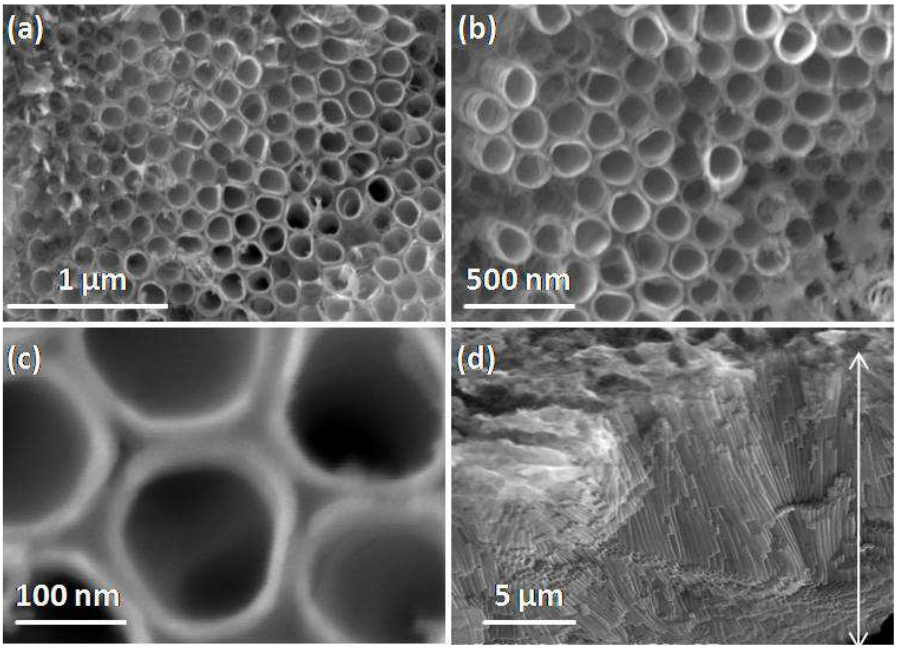

Fig. 3 FESEM images of TiO_2 NTs (a-c) top view and (d) cross-sectional view

Table 1 Summary of physical properties of TiO_2 NTs

Sample	Tube length (µm)	Wall thickness (nm)	Pore diameter (nm)
PT	14.1	22	110
GT	16.9	19	130

3.3 EDX analysis

EDX spectra were recorded for the synthesized TiO_2 NTs to identify the chemical composition. The EDX spectra of PT and GT are shown in Fig. 4 (a) and (b), respectively. As seen from the spectra, the elemental presence of Ti and O were confirmed [20]. The absence of impurity peaks indicates the high purity of the samples obtained by both the modes.

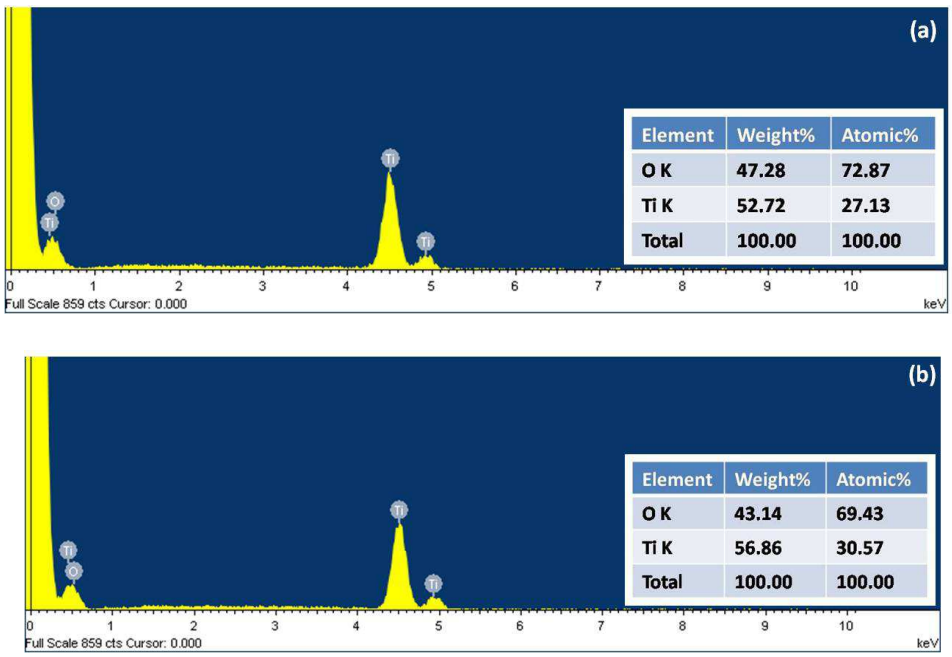

Fig. 4 EDX spectra of TiO_2 NTs (a) PT and (b) GT

3.4 FT-IR analysis

Fig. 5 shows the FT-IR spectra of the TiO_2 NTs (a) PT and (b) GT. The broad bands observed around 3200-3450 cm^{-1} and peaks around 1630 cm^{-1} are assigned to the stretching and bending vibrations of hydroxyl (O–H) group which is from the absorbed water on the TiO_2 surface. The bands around 2340 cm^{-1} correspond to the stretching and bending modes of C–H bonds. The bands around 450-800 cm^{-1} corresponds to the Ti-O bending mode of TiO_2. The observed results are in agreement with the earlier reports [21].

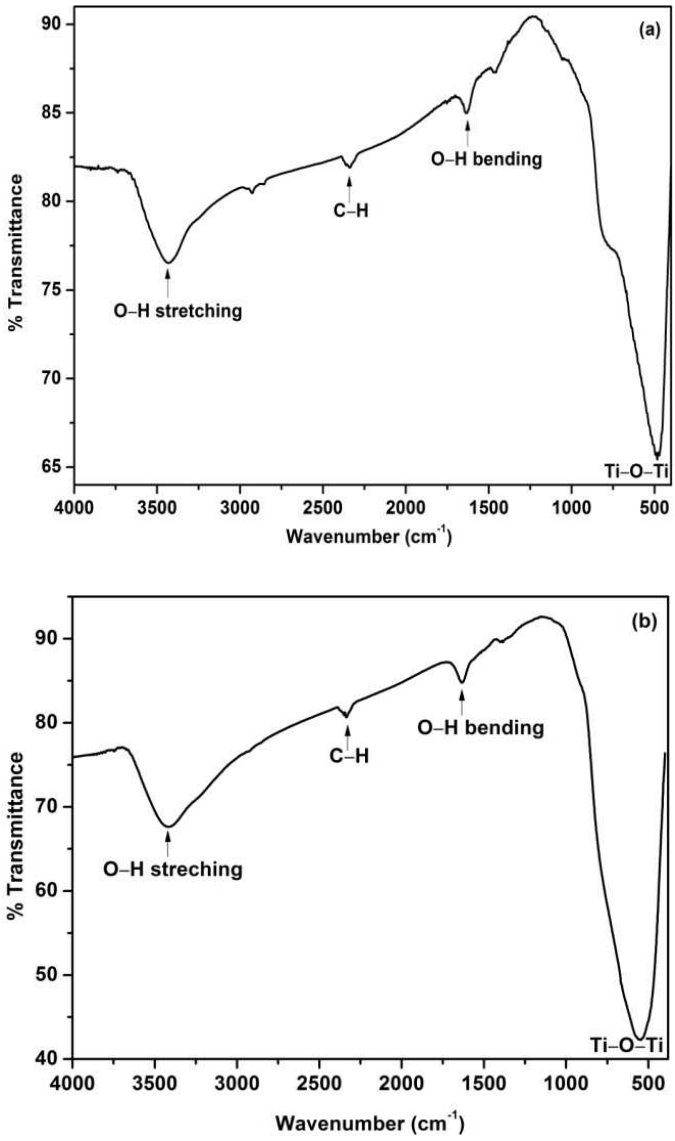

Fig. 5 FT-IR spectra of TiO_2 NTs (a) PT and (b) GT

4. 1 Cyclic voltammetry

The electrochemical performance of TiO_2 NTs as electrode for supercapacitor was investigated by cyclic voltammetry. Fig. 6 shows the CV curves for PT and GT electrodes collected at different scan rates over the wide range from 10 to 100 mV/s in 1 M Na_2SO_4 aqueous solution. Both the samples exhibit ideal rectangular shape CV curves, which is evidence of typical characteristic of double-layer capacitance. Absence of redox peaks suggests that the capacitive behavior is mainly due to ion adsorption onto the surface TiO_2 NTs [16]. These CV curves retain the rectangular shape even at the scan rate up to 100 mV/s, indicating good capacitive behavior and fast reaction rate. As the scan rate increases, the integrated area of the curves increases. The variation in current response at high scan rate is owing to electric polarization [22]. It is believed that the electrochemical performances are governed by the charge transfer kinetics and diffusion of electrolyte ions, which are dependent on the geometrical parameters. In comparison, the GT sample with enhanced geometrical parameters demonstrates improved performance than the PT sample.

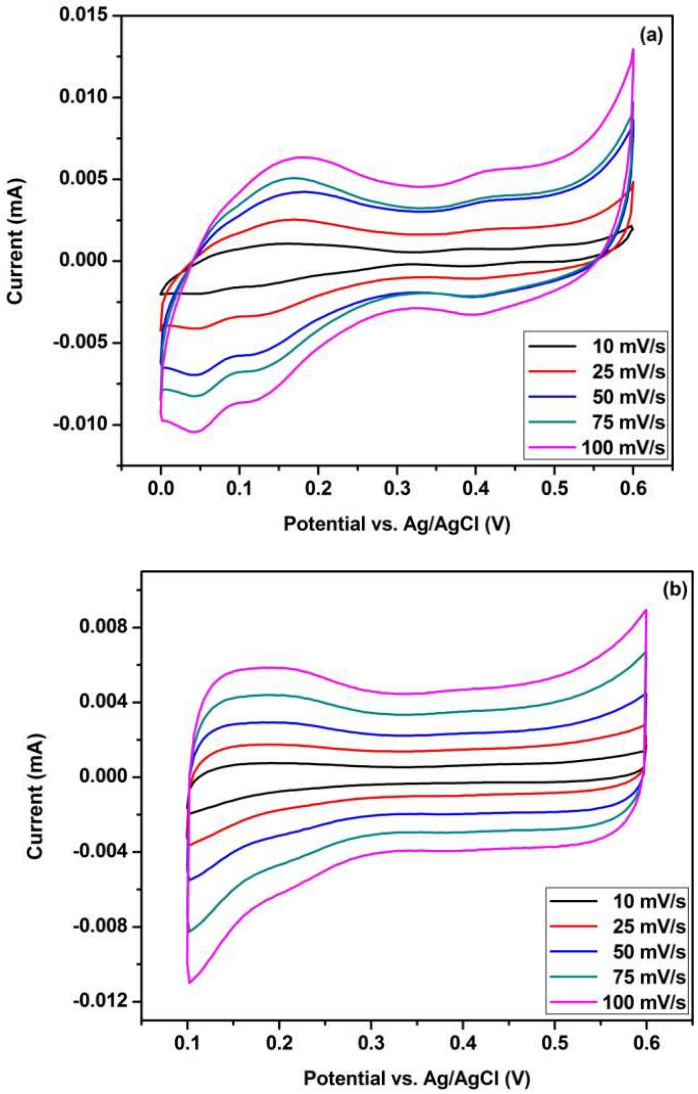

Fig. 6 Cyclic voltammograms of TiO_2 NTs (a) PT and (b) GT

4.2 Chronopotentiometry

The galvanostatic charge-discharge tests for the TiO_2 NTs electrodes were also conducted at different current densities as shown in Fig. 7. The smooth and symmetrical curves confirm great capacitive behavior of the electrodes. Specific capacitance of the samples can be calculated from the charge-discharge study using below equation:

$$SC = \frac{I \times t_d}{m \times \Delta V}$$

Where, I is the constant current applied, t_d is the discharge time, m is the mass of the material loaded and ΔV is the potential difference [22]. Specific capacitances of the samples calculated at 1 mA/g are found to be 24.4 mF/g and 27.1 mF/g for PT and GT, respectively. The enhanced capacitive behavior is attributed to unique nanotubular morphology and high surface area of TiO_2 NTs. Further, it could be increased by carefully tuning diameter and length of TiO_2 NTs.

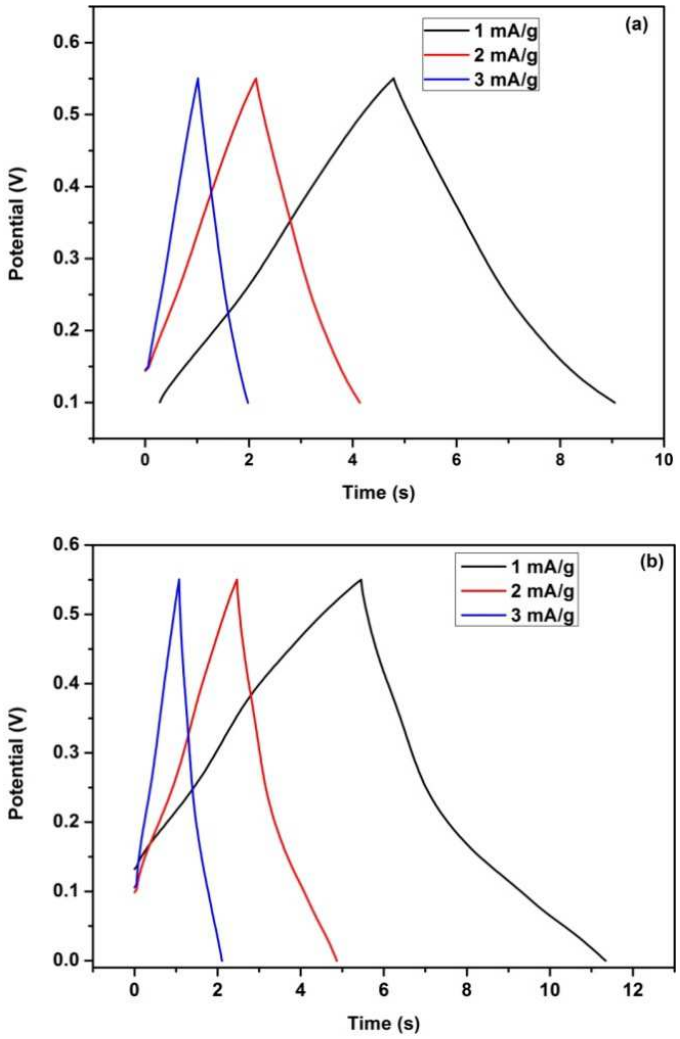

Fig. 7 Charge-discharge voltage profiles of TiO_2 NTs (a) PT and (b) GT

4.3 Electrochemical impedance spectroscopy

Electrochemical impedance spectroscopy (EIS) is subsequently used to evaluate the electrical conductivity and capacitive characteristics of electrode materials. The EIS measurements were carried out over a frequency range of 1 MHz to 1 Hz with AC signal amplitude of 10 mV. Fig. 8 presents Nyquist plots of TiO_2 NTs electrodes, where Z' and Z" are real and imaginary components of the impedance, respectively. Generally, the Nyquist plot of the electrochemical supercapacitor is composed of a high frequency semicircle and a low frequency nearly vertical line [23]. At high frequency region, intercept at real part of the axis gives equivalent series resistance (ESR) which is an aggregation of contributions from (i) discontinuity in the charge transfer process at the solid oxide/ liquid electrolyte interface (ii) intrinsic resistance of the oxides (iii) contact resistance between the active material and current collector and (iv) resistance due to the faradic process [22,23].

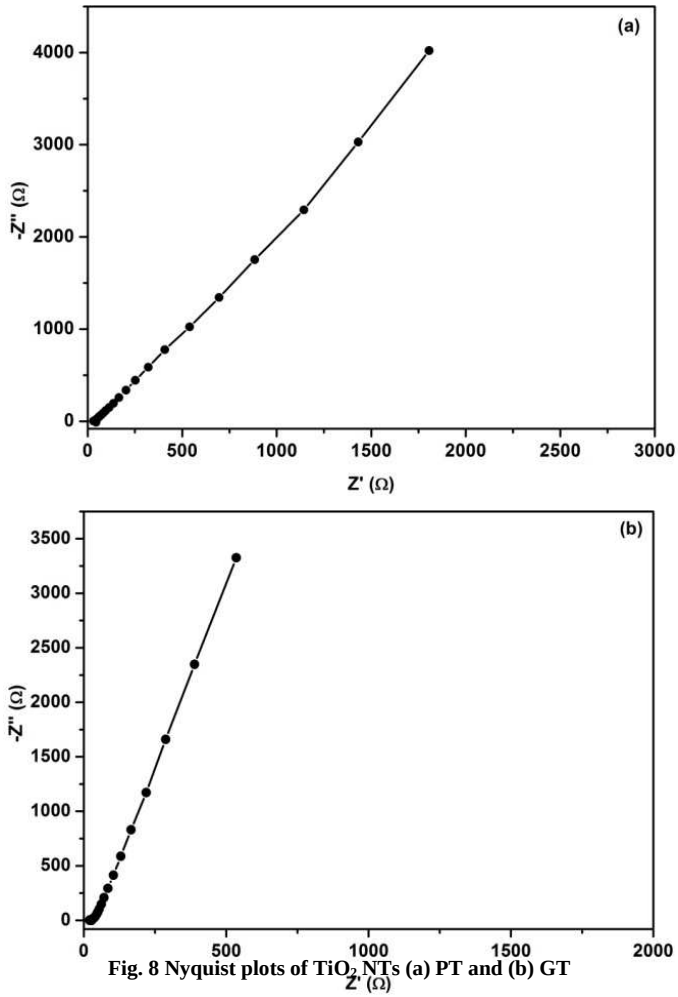

Fig. 8 Nyquist plots of TiO_2 NTs (a) PT and (b) GT

It is seen from the Fig. 8 that absence of semicircle in the high frequency region demonstrate low internal resistance of the electrode materials. Slope of the line at the low frequency region represents the diffusion resistance or Warburg impedance. The GT sample with higher slope value indicates the rapid ion transport within the pores of the electrode material.

CONCLUSION

Self-organized TiO_2 NTs were successfully fabricated via potentiostatic and galvanostatic anodization approaches. The sample prepared by galvanostatic mode demonstrated enhanced capacitive behavior than the sample prepared by potentiostatic mode. The observed electrochemical results suggest that the TiO_2 NTs could serve as promising electrode material for supercapacitor applications.

Acknowledgement
The authors acknowledge Loyola College-Times of India (LC-TOI) Research Initiative (Ref. No. 3LCTOI14PHY001) for funding this research work and for providing the research facility at the Department of Physics, Loyola College (Autonomous), Chennai-600034.

REFERENCES

[1] Yu Z, Tetard L, Zhai L and Thomas J, *Energy Environ. Sci*., **2015**, 8, 702-730.
[2] Narayanan R, Naresh Kumar P, Deepa M and Srivastava AK, *Electrochimica Acta*, **2015**, 178, 113-126.
[3] Simon P and Gogotsi Y, *Nature Materials*, **2008**, 7, 845-854.
[4] Huang YG, Zhang XH, Chen XB, Wang HQ, Chen JR, Zhong XX and Li QY, *Int. J. Hydrogen Energy*, **2015**, 40, 14331-14337.
[5] Zhou M, Glushenkov AM, Kartachova O, Li Y and Chena Y, *J. Electrochem. Soc*., **2015**, 162, A5065-A5069.
[6] Dar FI, Moonooswamy KR and Es-Souni M, *Nanoscale Res. Lett*., **2013**, 8, 363-369.
[7] Wang YG, Wang ZD and Xia YY, *Electrochimica Acta*, **2005**, 50, 5641-5646.
[8] Roy P, Kim D, Lee K, Spiecker E and Schmuk P, *Nanoscale*, **2010**, 2, 45-59.

[9] Manovah David T, Sagayaraj P, Wilson P, Ramesh C, Murugesan N, Prabhu E, Murthy ASR and Annapoorani, *J. Electrochem. Soc*., **2016,** 163, B15-B18.
[10] Wu QL, Li J, Deshpande RD, Subramanian N, Rankin SE, Yang F and Cheng YT, *J. Phys. Chem. C*, **2012**, 116, 18669-18677.
[11] Xiong H, Slater MD, Balasubramanian M, Johnson CS and Rajh T, *J. Phys. Chem. Lett*. **2011**, 2, 2560-2565.
[12] Salari M, Aboutalebi SH, Konstantinov K and Liu HK, *Phys. Chem. Chem. Phys*., **2011**, 13, 5038-5041.
[13] Clement Raj C, Sundheep R and Prasanth R, *Electrochimica Acta*, **2015**, 176, 1214-1220.
[14] Endut Z, Hamdi M and Basirun WJ, *Surf. Coat. Tech*., **2013**, 215, 75-78.
[15] Xiao P, Zhang Y, Garcia BB, Sepehri S, Liu D and Cao G, *J. Nanosci. Nanotech*., **2008**, 8, 1-11.
[16] Tamilselvan A and Balakumar S, *Ionics*, **2016**, 22, 99-105.
[17] Kim MS, Lee TW and Parka JH, *J. Electrochem. Soc*., **2009**, 156, A584-A588.
[18] Jun Y, Parkw JH and Kang MG, *Chem. Commun*., **2012**, 48, 6456-6471.
[19] Zhang H, Chen Z, Song Y, Yin M, Li D, Zhu X, Chen X, Chang PC and Lu L, *Electrochem. Commun*. **2016**, 68, 23-27.
[20] Shibu Joseph and Sagayaraj P, *New J. Chem.*, **2015**, 39, 5402-5409.
[21] Antony RP, Mathews T, Dash S, Tyagi AK, Raj B, *Mater. Chem. Phy*., **2012**, 132, 957-966.
[22] Naveen AN and Selladurai S, *Electrochemica Acta*, **2015**, 173, 290-301.
[23] Wu H, Li D, Zhu X, Yang C, Liu D, Chen X, Song Y and Lu L, *Electrochimica Acta*, **2014**, 116, 129-136.